ELSEVIER

Catalysis Today 78 (2003) 229–236

CATALYSIS TODAY

www.elsevier.com/locate/cattod

Thermal behaviour, redox properties, and catalytic performance of alkali-promoted V_2O_5 catalysts in the selective oxidation of *p*-methoxytoluene: a comparative study

Ursula Bentrup*, Andreas Martin, Gert-Ulrich Wolf

Institut für Angewandte Chemie Berlin-Adlershof e.V., Richard-Willstätter-Str. 12, D-12489 Berlin, Germany

Abstract

Alkali-promoted V_2O_5 catalysts M–V_2O_5 (M = Li, K, Cs) were synthesised by impregnation of V_2O_5 with alkali sulphate solution. Pure V_2O_5 was used for comparison. X-ray diffraction, spectroscopic (FTIR), and thermoanalytical methods (STA/MS) have been used to characterise the phase composition, the adsorption properties, and the reducibility of the catalysts. The catalytic performance was proved using the oxidation of *p*-methoxytoluene (PMT) to *p*-methoxybenzaldehyde (PMBA) as test reaction. The surface acidity is lowered, but the reducibility is enhanced with increasing size and basic properties of the alkali cation. This leads to an increased adduct (PMT) adsorption and decreased product (PMBA) adsorption in the order V_2O_5 < Li–V_2O_5 ≪ K–V_2O_5 < Cs–V_2O_5. Consequently, the catalytic performance is improved in the same way. The formation of bronze phases at relative low temperatures in the case of K– and Cs–V_2O_5 stabilise V^{4+} oxidation state and improve the redox properties and consequently the catalytic results. The admixture of the non-reactive pyridine enhances the aldehyde selectivity by further lowering of the surface acidity. Additionally, pyridinium cations generated during catalytic reaction and incorporated into the formed alkali bronze phases stabilise these structures.

Keywords: V_2O_5 catalysts; Alkali-promotion; Selective oxidation; Thermal analysis; FTIR; XRD

1. Introduction

Especially *p*-substituted benzaldehydes are important intermediates in the field of speciality and pharmaceutical chemicals which can be prepared by several conventional methods, mainly in the liquid phase [1–3]. However, there are several advantages for a vapour phase catalytic oxidation process. But, it has to be taken into account that the selective production of aromatic aldehydes in vapour phase processes is more complicated due to a faster consecutive oxidation of the aldehydes to acids and deeper oxidised products.

Some work has been done in the last two decades in the field of the oxidation of methyl aromatics to their corresponding aldehydes in the vapour phase to get a deeper knowledge and insight into reactant–catalyst interaction by the application of various in situ methods (e.g. [4–6]) and to find promising new catalyst compositions.

Mainly Japanese groups reported on the role of acid and base properties of vanadium oxide catalysts containing basic metal oxides (M = K, Rb, Cs, Tl, Ag) for the partial oxidation of methyl aromatics to their corresponding aldehydes (e.g. [7]). They stated that the selectivity to substituted benzaldehydes is

* Corresponding author. Fax: +49-30-6392-4350.
E-mail address: bentrup@aca-berlin.de (U. Bentrup).

0920-5861/02/$ – see front matter
PII: S0920-5861(02)00344-9

closely related to the basic properties of the catalyst whereas the activity strongly depends on the amount and strength of acid sites.

These findings agree with the results of our studies on the oxidation of methyl aromatics to their corresponding benzaldehydes on the rather acidic $(VO)_2P_2O_7$ catalyst [6,8]. It was found that mainly Brønsted acid OH-groups formed during the reaction by interaction of V–O–P bonds with water are responsible for a restricted aldehyde desorption which leads to poor aldehyde selectivities by consecutive over-oxidation. The addition of the non-reactive base pyridine to the feed significantly improves the aldehyde selectivity by an effective blockade of these acidic sites [8].

The application of vanadium oxide (V_2O_5) catalysts in partial oxidation reactions is widely practised. Several studies were carried out to investigate the promotion effect of alkali compounds or basic oxides to V_2O_5 on the catalytic performance in different reactions (e.g. [9–14]). Generally, the promotion of V_2O_5 bulk and supported catalysts with alkali compounds improves the selectivity to partial oxidation products. The doping effect of mainly potassium compounds has been explained: (i) by the lowering of the acid sites and/or (ii) by changing the redox properties of the catalysts. Furthermore, the potassium addition influences the surface concentration of electrophilic oxygen, which is responsible for deep oxidation, and the concentration of nucleophilic oxygen, responsible for the partial oxidation [13].

Recent studies of the partial oxidation of substituted toluenes to their corresponding aldehydes on alkali metal-containing vanadia catalysts have shown [14] that toluene conversion and aldehyde selectivity change with alkali cation size. Increasing cation size and consequently increasing basicity in the order from Li to Cs causes declining toluene conversion but increasing aldehyde selectivity. Further investigations of these catalysts revealed [15] that the onset temperatures of the reduction decrease in the order $V_2O_5 > Li–V_2O_5 \gg K–V_2O_5 \approx Cs–V_2O_5$. The ability to form crystalline mixed-valence bronze-like phases $M_xV_2O_5$ ($x = 0.2–0.5$) beside V_2O_5 increases in the same order. It was assumed that the bronze phases stabilise V^{4+} oxidation state and improve the redox properties.

It is the aim of this work to elucidate the relationship between specific catalyst properties induced by alkali metal promotion and the catalytic performance of these catalysts in the partial oxidation of *p*-methoxytoluene (PMT) to *p*-methoxybenzaldehyde (PMBA). Thermoanalytical methods, FTIR spectroscopy and X-ray diffraction (XRD) were applied to study adsorption properties, redox behaviour, and phase-transformations during catalytic tests.

2. Experimental

2.1. Catalysts

$M–V_2O_5$ catalysts were prepared by incipient wetness method with an aqueous M_2SO_4 (M = Li, Na, K, Rb, Cs) solution. The 50 ml of such a solution (0.01 mol M_2SO_4) were added to 0.1 mol V_2O_5 (Gesellschaft f. Elektrometallurgie Nürnberg) and evaporated using a rotary evaporator at 70 °C for 1 h. A further evaporation to dryness was carried out under vacuum at this temperature. The obtained product was dried overnight at 130 °C. For comparison, pure V_2O_5 was treated by the same procedure using distilled water. The obtained samples were characterised by XRD and FTIR spectroscopy as described elsewhere [14,15].

2.2. FTIR experiments

Spectra were recorded using a Bruker IFS 66 spectrometer equipped with a heatable and evacuable IR cell with CaF_2 windows, connected to a gas dosing/evacuation system. For the experiments the catalyst powders were pressed into self-supporting discs with a diameter of 20 mm and a weight of 50 mg and activated by heating up to 400 °C (V_2O_5, $Li–V_2O_5$) and 300 °C ($K–V_2O_5$, $Cs–V_2O_5$) in Ar followed by cooling to room temperature.

For the investigations under reaction-like conditions the feed composition (molar ratios) was PMT:air = 1:225. The PMT was fed with argon using a saturator heated to 60 °C. Additional dosage of argon provided a constant gas flow of 11.4 l/h. The adsorption spectra were recorded at the reaction temperature (300 °C). The figures show difference spectra obtained by subtraction of the spectrum of the activated catalyst at 300 °C.

2.3. Thermal analysis

Simultaneous thermal analytical (STA) measurements (TG and DTA) were carried out on a Netzsch STA 409 thermoanalyser connected by a heated stainless steel capillary to a Balzers quadrupole mass spectrometer QMG 420.

For the standard experiments the samples (20–25 mg) were heated in helium (3 l/h) with a heating rate of 10 °C/min using Al_2O_3 crucibles. The reference material was Al_2O_3. The desorption experiments of PMT were carried out after ex situ adsorption of PMT at room temperature.

2.4. Catalytic measurements

For the catalytic tests a microreactor set-up containing a metering system for liquids and gases and a fixed bed quartz glass reactor were used. The catalysts were introduced into the reactor as sieve fractions (1–1.25 mm) and mixed prior to oxidation runs with the equal portion of quartz glass (1 mm) to avoid local overheating. The product stream was analysed by on line GC or it was trapped in aqueous ethanol and determined by off line capillary GC. The formation of carbon oxides was continuously followed by non-dispersive IR photometry.

3. Results and discussion

Exemplarily, the FTIR spectra obtained during the reaction of PMT/air on the V_2O_5 and Cs–V_2O_5 catalysts at 300 °C for 60 min are depicted in Fig. 1. The spectra were measured at intervals of 15 min. During adsorption of PMT/air on V_2O_5 (Fig. 1a), besides the aromatic ring vibrations around 1600 cm^{-1} additional bands were observed at about 1672, 1739, 1782 and 1855 cm^{-1}. The band at 1672 cm^{-1} is most likely due to the C=O group of adsorbed coordinatively bonded benzaldehyde, whereas the bands at 1739, 1782 and 1855 cm^{-1} are caused by cyclic anhydride species physically adsorbed on the surface [16,17]. Such anhydrides may be generated by an oxidative attack on the aromatic nucleus and have to be considered as intermediates on the way to total oxidation. As shown in earlier studies [6,8,17], especially Brønsted acid hydroxyl groups cause the strong adsorption of the

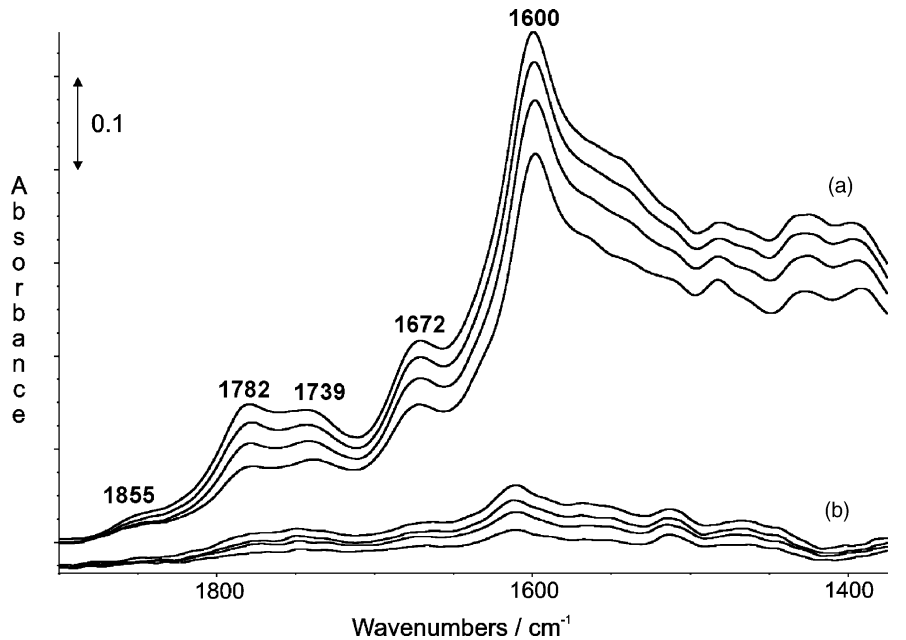

Fig. 1. Reaction of PMT/air (molar ratio: 1:225) at 300 °C on V_2O_5 (a) and Cs–V_2O_5 (b). FTIR spectra obtained after 15, 30, 45 and 60 min (from bottom to top) contact time, respectively.

aldehyde leading to deeper oxidation products. It is clearly seen from comparison of Fig. 1a and b that the amount of adsorbed aldehyde and anhydride is much lower in the case of Cs–V_2O_5 which is caused by the essential lower surface acidity compared with that of pure V_2O_5. This effect of decreasing surface acidity with increasing size and basic properties of the promoting alkali cation has been proved by adsorption of pyridine [15]. The appearance of adsorbed benzaldehyde is always accompanied by that of adsorbed cyclic anhydride. By comparing the band intensities of both adsorbed species, it is obvious that the amount of adsorbed anhydride grows up faster with reaction time than that of adsorbed aldehyde. This finding reflects the consecutive oxidation caused by the strong product adsorption on the catalyst surface. Lowering of the surface acidity leads to a decreased aldehyde adsorption and consequently, the formation of cyclic anhydrides is suppressed and the aldehyde selectivity is improved. This effect was also found in the case of Li–V_2O_5 and K–V_2O_5.

Besides the adsorption and desorption behaviour of the product benzaldehyde, the chemical behaviour of the adduct PMT also influences the catalytic performance. As known from earlier studies [6], PMT is strongly adsorbed at the catalyst surface of vanadyl pyrophosphate (VPP). The desorption and reaction of PMT adsorbed on V_2O_5 and alkali-promoted V_2O_5 catalysts was investigated by STA coupled with mass spectrometric analysis of the evolved gases. The TG and ion current curves of the typical fragment with mass number 77 for PMT measured for V_2O_5, Li–V_2O_5, K–V_2O_5, and Cs–V_2O_5 in the temperature range 30–200 °C are shown in Fig. 2A. The TG and ion current curves of the mass number 44 (CO_2) in the temperature range 20–500 °C are presented in Fig. 2B. It has to be mentioned that in addition to PMT some water is evolved up to 250 °C. The amount of adsorbed PMT increases in the order V_2O_5 < Li–V_2O_5 ≪ K–V_2O_5 < Cs–V_2O_5 (Fig. 2A). As can be seen from the maxima of desorption temperature, the strength of adsorption is the highest for Cs–V_2O_5. In the temperature range 200–450 °C the evolution of CO_2 can be observed (Fig. 2B) caused by the oxidation of chemisorbed PMT and/or adsorbed aldehyde formed during heating. The formation of CO_2 is accompanied by a exothermic DTA effect (not shown in the figure) which is strong in the case of K–V_2O_5. It is obvious that the ability for adsorbing PMT facilitates the formation of oxidation products. Moreover, this oxidation power of the different catalysts correlates with their reducibility. This finding is in line with the results recently reported in [15]. The onset temperatures of the reduction decrease in the order V_2O_5 > Li–V_2O_5 ≫ K–V_2O_5 ≈ Cs–V_2O_5. That means, the reducibility is higher for K– and Cs–V_2O_5 than for Li–V_2O_5 and V_2O_5. In this connection it was also found that the tendency to form mixed-valence bronze phases $M_xV_2O_5$ ($x = 0.2$–0.5) is essentially more pronounced in the case of M = K, Cs than for M = Li because K– and Cs–bronze phases are formed at lower temperatures.

The catalytic tests of the partial oxidation of PMT to PMBA were carried out at 355–365 °C. Concerning the selectivity enhancing effect of pyridine admixture [8] in the case of VPP catalysts, the experiments were performed without and with pyridine in the feed. The results of the catalytic tests are summarised in Fig. 3. For comparison, the results obtained with VPP are incorporated in the diagram. It is clearly shown that the alkali-promoted V_2O_5 catalysts exhibit essentially higher conversion and higher PMBA selectivities. Obviously, the vanadia catalysts are more active than the VPP catalysts. Whereas on pure V_2O_5 high conversion of about 75% was observed the selectivity of 10–15% was rather low. A similar behaviour was found for Li–V_2O_5. However, the promotion of V_2O_5 with potassium or caesium leads to lower conversion of 40–50% but much higher selectivities than for Li–V_2O_5 (Fig. 3).

Whereas the admixture of pyridine in the case of VPP has no effect, the PMBA selectivities in the case of the vanadia catalysts were dramatically increased, especially for K–V_2O_5 and Cs–V_2O_5. The conversion was a little bit lower for Li–V_2O_5 and K–V_2O_5, but not for Cs–V_2O_5. Earlier investigations [14] have shown that the composition of the K– and Cs–V_2O_5 catalysts changes after catalytic reaction without pyridine. Mixed-valence bronze phases like $K_{0.5}V_2O_5$ and $Cs_{0.3}V_2O_5$ were detected besides V_2O_5. Depending on the reaction conditions (mainly oxygen content and reaction time) also another potassium containing compound $K_{0.24}V_2O_5$ was identified.

The XRD patterns of the different samples used in catalytic reaction with pyridine are presented in Fig. 4. The catalysts V_2O_5 and Li–V_2O_5 remained

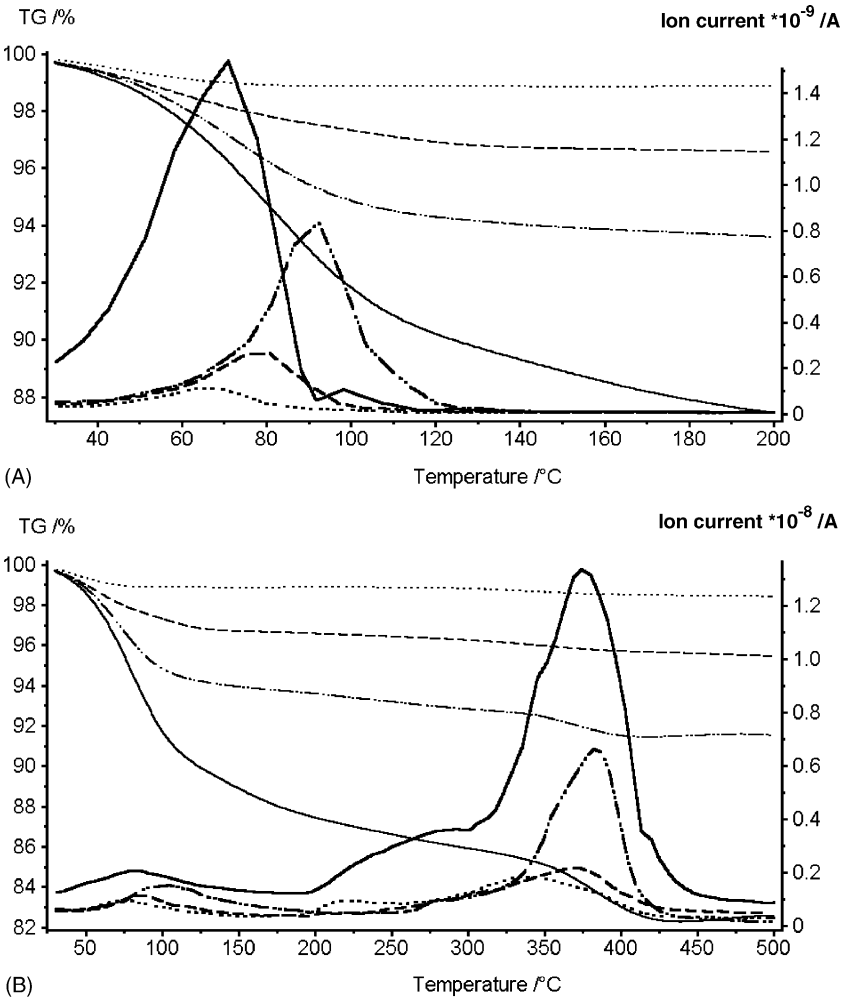

Fig. 2. TG and ion current curves of mass number 77 (PMT) (A) and mass number 44 (CO_2) (B) of V_2O_5 (···), Li–V_2O_5 (---), K–V_2O_5 (—), and Cs–V_2O_5 (–···–) after ex situ adsorption of PMT.

unchanged (Fig. 4a and b), only the peaks for V_2O_5 could be detected. Additional peaks around $d = 1060$ and 1270 pm ($2\Theta = 8.34$ and 6.95) appeared in the case of K–V_2O_5 and Cs–V_2O_5 (Fig. 4c and d). These *d*-values are higher than that for the strongest peak of $K_{0.5}V_2O_5$ with $d = 940$ pm. No peaks for $K_{0.5}V_2O_5$ and the hexagonal $Cs_{0.3}V_2O_5$ were detected. This finding can be explained by the assumption that pyridine is incorporated into the layer structure of V_2O_5 and, hence, prevents the formation of such phases. The powder diffraction pattern of a separate prepared pyridinium vanadate phase with the approximate composition $PyH_{0.7}V_2O_5$, exhibited also the strongest peak at $d = 1080$ pm ($2\Theta = 8.18$) [18]. Considering the formation of a similar layer structure that exists in $K_{0.5}V_2O_5$, the incorporation of pyridine should expand the distance of the layers within the structure. Consequently, the strongest peak indicated the layer distance is shifted to higher *d*-values.

Furthermore, it was found that the expansion of the layers obviously depends on the concentration of pyridine in the feed. The XRD patterns of K–V_2O_5 samples obtained after different catalytic tests are also depicted in Fig. 4. Whereas the pattern

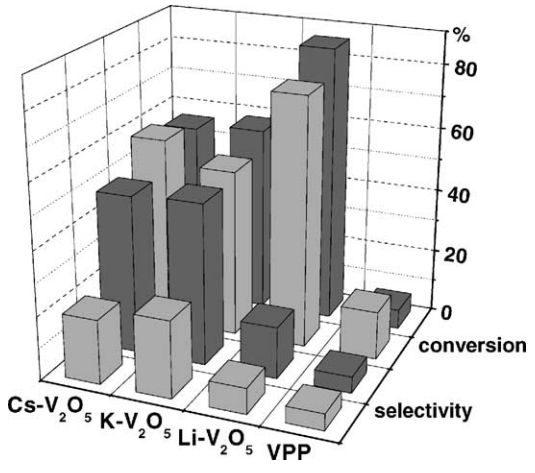

Fig. 3. Conversion and selectivity of PMBA without pyridine (light grey) and with pyridine (dark grey) on Li–V_2O_5, K–V_2O_5, Cs–V_2O_5 and VPP under the following reaction conditions: $T = 355$–$365\,^{\circ}C$; PMT:O_2:N_2:H_2O:pyridine = 1:72:256:21:5.

c was observed after catalytic test with high concentration of pyridine (PMT:O_2:N_2:pyridine:H_2O = 1:84:290:32:145), pattern e was obtained after catalytic reaction with low pyridine concentration in the feed (PMT:O_2:N_2:pyridine:H_2O = 1:72:256:5:21). Pattern f was obtained after several catalytic tests with different concentrations of oxygen and pyridine. It is obvious that with higher concentration of pyridine the two peaks in addition to the typical peaks of V_2O_5, shift from $d = 950$ and 1070 pm ($2\Theta = 9.34$ and 8.22) (Fig. 4e) to $d = 1060$ and 1270 pm ($2\Theta = 8.34$ and 6.95) (Fig. 4c). The pattern of the catalyst from the long-term experiment (Fig. 4f) exhibits peaks from V_2O_5, the bronze phase $K_{0.24}V_2O_5$ [15], and one additional peak at about $d = 1270$ pm ($2\Theta = 6.95$). Evidently, the different reaction conditions and/or the longer use of the catalyst led to a more reduced sample. The additional formation of $K_{0.24}V_2O_5$ indicates a higher reduction degree of the sample. The peak at $d = 1270$ pm ($2\Theta = 6.95$) is obviously due to a pyridinium containing bronze phase.

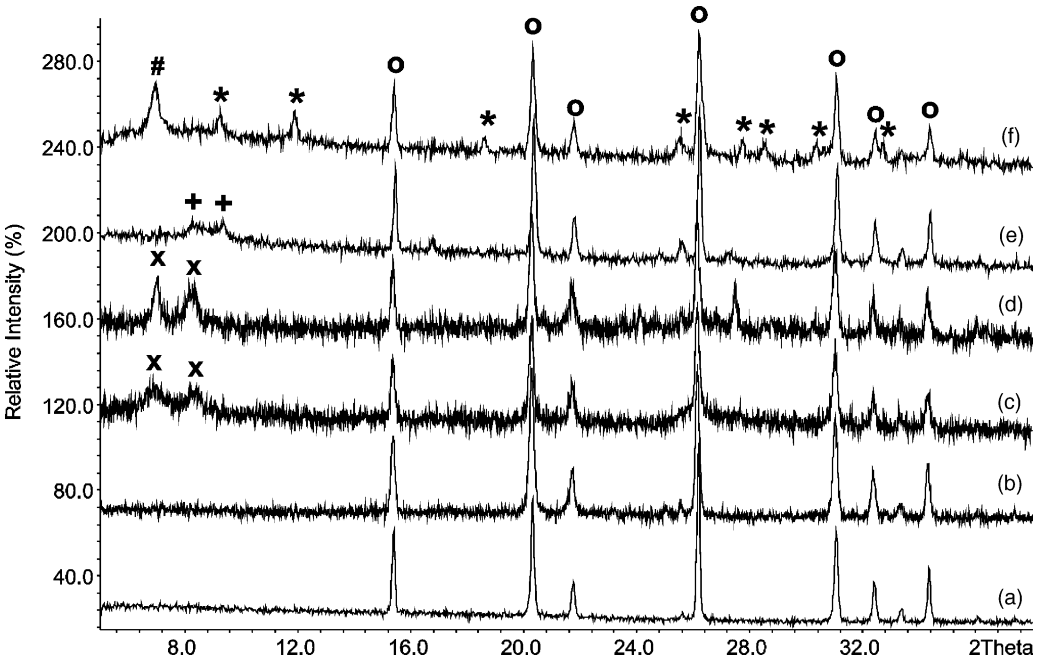

Fig. 4. XRD patterns of: (a) V_2O_5; (b) Li–V_2O_5; (c) K–V_2O_5; (d) Cs–V_2O_5 catalysts used during oxidation of PMT with high pyridine concentration (PMT:O_2:N_2:H_2O:pyridine = 1:84:290:145:32); (e) K–V_2O_5 used during oxidation with low pyridine concentration (PMT:O_2:N_2:H_2O:pyridine = 1:72:256:21:5); (f) K–V_2O_5 used during several catalytic tests with and without pyridine. (○) V_2O_5, (∗) $K_{0.24}V_2O_5$, (×, +, #) unknown vanadate phases.

Checking the correctness of this assumption, the $Li–V_2O_5$, $K–V_2O_5$ (after short and longer use), and $Cs–V_2O_5$ catalyst tested in reactions with pyridine-containing feed were investigated by STA coupled with mass spectrometric analysis. The ion current curves of the mass number 52 (representative for pyridine) are shown in Fig. 5A, the curves of the mass number 44 (CO_2) are represented in Fig. 5B. From the decomposition of pyridinium vanadate $PyH_{0.7}V_2O_5$ it is known that one part of pyridine is evolved in the temperature range 200–400 °C, whereas the remaining part is oxidised around 400 °C forming CO_2 [18]. As can be seen from Fig. 5A most of the pyridine is evolved from K– and $Cs–V_2O_5$ catalysts between 100 and 180 °C. No pyridine was detected in the case of $Li–V_2O_5$ which supports the assumption that no pyridine is incorporated. Additionally, the oxidation of pyridine can be observed as indicated by formation of CO_2. Whereas pyridine from $Cs–V_2O_5$ is oxidised between 180 and 400 °C (Fig. 5B), the pyridine

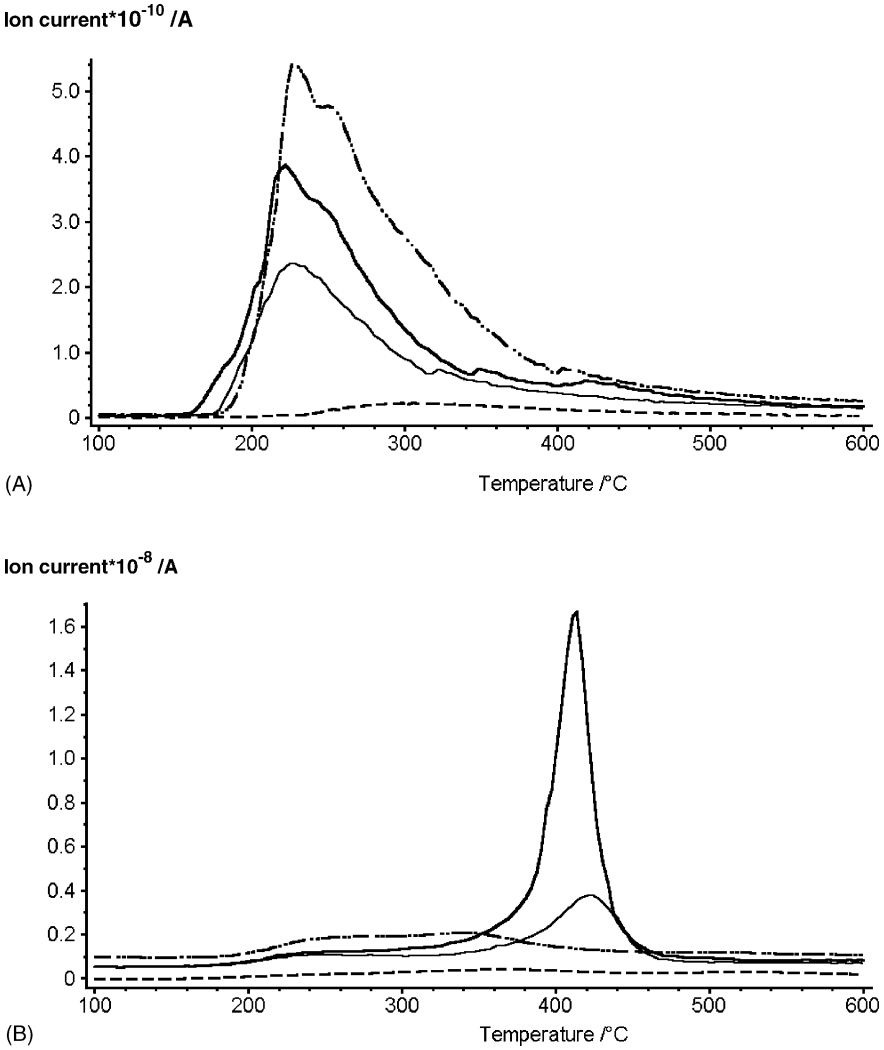

Fig. 5. Ion current curves of pyridine (mass number 52) (A) and CO_2 (mass number 44) (B) of $Li–V_2O_5$ (- - -), $K–V_2O_5$ (—), $K–V_2O_5$, longer used (—), and $Cs–V_2O_5$ (– ⋯ –) catalysts used during oxidation of PMT in the presence of pyridine.

incorporated in the K–V_2O_5 catalysts seems to be more stable because the last proportion is evolved as CO_2 above 400 °C.

After these thermoanalytical experiments the powder diffraction patterns of K– and Cs–V_2O_5 catalysts showed only peaks of $K_{0.5}V_2O_5$ and $Cs_{0.3}V_2O_5$, respectively, in addition to the peaks of V_2O_5. After decomposition of the pure pyridinium vanadate $PyH_{0.7}V_2O_5$ only peaks of V_2O_5 were detected in the XRD pattern [18]. Consequently, these experiments confirmed the assumption that obviously mixed-valence pyridinium alkali vanadates with bronze-like structures are formed during the catalytic experiment. These pyridinium vanadates are characterised by similar structures known from the respective alkali vanadia compounds. Obviously, the formation of alkali bronze phases seems to be the supposition for the incorporation of pyridinium ions in the structure under the specific conditions of the catalytic reaction.

4. Conclusions

The alkali-promotion of V_2O_5 effects new surface arrangements of vanadyl groups and influences the surface acidity and reducibility of the catalysts. The surface acidity is lowered with increasing size and basic properties of the alkali cation. Lowering of the surface acidity leads to an increased adduct (PMT) adsorption in the order V_2O_5 < Li–V_2O_5 ≪ K–V_2O_5 < Cs–V_2O_5, whereas the product (PMBA) adsorption is decreased in the same order. The ability for adsorbing PMT facilitates the formation of oxidation products. This oxidation power of the different catalysts correlates with their reducibility.

Alkali-promoted V_2O_5 catalysts exhibit essentially higher conversion and higher PMBA selectivities than VPP catalysts which is caused by their lower surface acidity and better redox properties indicated by the formation of mixed-valence alkali vanadia bronze phases during reaction.

The admixture of pyridine improves the catalytic results especially for K–V_2O_5 and Cs–V_2O_5. This effect is caused by a further and permanent lowering of surface acidity during catalytic reaction. Additionally, pyridinium cations generated during reaction are able to incorporate into the structure of alkali vanadia bronze phases. These mixed-valence bronze phases stabilise V^{4+} oxidation state and improve the redox properties. The potassium-promoted vanadia catalyst revealed the best catalytic results, obviously caused by the efficient combination of low surface acidity and high reducibility realised by the structural variability of the potassium vanadia bronzes.

Acknowledgements

The authors thank Mrs. U. Wolf, Mrs. I. Kurzawski and Mrs. H. French for experimental assistance, Dr. H. Berndt for discussions, and the Federal Ministry of Education and Research, Germany, for financial support (project no. 03C0280).

References

[1] T. Tzedakis, A.J. Savall, Ind. Eng. Chem. Res. 31 (1992) 2475.
[2] R.A. Sheldon, N. de Heij, Stud. Org. Chem. 33 (1988) 234.
[3] F. Brühne, E. Wright, in: Ullmann (Ed.), Electronic Release, 6th ed., 1998 (benzaldehyde entry).
[4] G. Centi, S. Perathoner, S. Tonini, Catal. Today 61 (2000) 211.
[5] D.A. Bulushev, L. Kiwi-Minsker, A. Renken, Catal. Today 57 (2000) 231.
[6] U. Bentrup, A. Brückner, A. Martin, B. Lücke, J. Mol. Catal. A 162 (2000) 383.
[7] M. Ueshima, N. Saito, N. Shimizu, Stud. Surf. Sci. Catal. 90 (1994) 59.
[8] A. Martin, U. Bentrup, B. Lücke, A. Brückner, Chem. Commun. (1999) 1169.
[9] B. Grzybowska-Swierkosz, Appl. Catal. A 157 (1997) 263.
[10] N. Shimizu, N. Saito, M. Ueshima, Successful Des. Catal. 44 (1988) 131.
[11] M. Ponzi, C. Duschatzky, A. Carrascull, E. Ponzi, Appl. Catal. A 169 (1998) 373.
[12] T. Ono, Y. Tanaka, T. Takeuchi, K. Yamamoto, J. Mol. Catal. A 159 (2000) 293.
[13] D.A. Bulushev, L. Kiwi-Minsker, V.I. Zaikovskii, O.B. Lapina, A.A. Ivanov, S.I. Reshetnikov, A. Renken, Appl. Catal. A 202 (2000) 243.
[14] A. Martin, U. Bentrup, G.-U. Wolf, Appl. Catal. A 227 (2002) 131.
[15] A. Martin, U. Bentrup, G.-U. Wolf, Thermochim. Acta, in press.
[16] A.J. van Hengstum, J. Pranger, S.M. van Hengstum-Nijhuis, J.G. van Ommen, P.J. Gellings, J. Catal. 101 (1986) 323.
[17] U. Bentrup, A. Martin, B. Lücke, Top. Catal. 11–12 (2000) 139.
[18] G.-U. Wolf, Unpublished results.